

# DIII-D Capabilities and Tools for Plasma Science Research

By the DIII-D Team, edited by D.M. Orlov and R.J. Buttery

Version 6, released Nov 2021

*This is a live document, updated as we augment the facility and our notes.*

## Summary:

DIII-D is a flexible plasma science research facility. It operates an open program to which members of the worldwide fusion community can propose ideas. Ideas are typically selected on the basis of their potential to advance the science, techniques and predictive capabilities for future fusion energy devices such as ITER, future nuclear science facilities or power plants. The research program thus also seeks to address foundational scientific questions behind fusion relevant plasma behavior.

The program represents a broad collaboration of ~95 participating institutions covering a wide range of topical areas, which are deemed important to understand for fusion and plasma science. Research tends to focus on aspects which are most important to these future devices, and also where the facility's contribution is most distinctive and needed. We are also exploring potential to address more basic plasma science questions relevant to other areas of plasma physics that are a priority in the US program.

The DIII-D program welcomes further participation, which can enhance the understanding of plasma physics. To this end we have compiled this Capabilities document, to help advise potential new users on what can be done with the facility. This is intended to be an evolving document, and we welcome suggestions and questions on what is most useful to include.

*As DIII-D is a continuously changing facility, with new capabilities being added every year, this document represents a snapshot of capabilities at the time of release. Further editions will be periodically released. For the latest picture it is always best to contact the relevant system responsible person directly, listed in this document.*

**DIII-D External Web Page for collaborators:** <https://fusion.gat.com/global/Home>

Remote participation (meetings): <https://diii-d.gat.com/diii-d/Remote>

Cyber access: <https://fusion.gat.com/global/computing>

## Index

1.	DIII-D Key Physics Parameters .....	5
2.	DIII-D Facility Specifications .....	5
2.1.	Tokamak Systems .....	5
2.1.1.	Non-axisymmetric magnetic perturbations.....	5
2.2.	Heating, Fueling and Control Systems:.....	6
2.2.1.	Neutral Beam Injection Systems:.....	6
2.2.3.	Helicon Ultra High Harmonic Fast Wave.....	8
2.2.4.	High Field Side Lower Hybrid Current Drive .....	8

2.3.	Pellet / Gas Systems .....	8
2.3.1.	Gas Injection .....	8
2.3.2.	Vacuum and Wall Conditioning.....	9
2.3.3.	Deuterium Pellet Injection: .....	9
2.3.4.	Laser Blow Off.....	9
2.3.5.	Impurity Granule Injector (IGI):.....	10
2.3.6.	Impurity Powder Dropper (IPD):.....	10
2.3.7.	Impurity Single Granule Dropper: .....	10
2.3.8.	Massive Gas Injection: .....	10
2.3.9.	Shattered Pellet Injection:.....	10
2.3.10.	Solid Argon pellet injector.....	10
2.3.11.	Shell pellet injector.....	11
2.4.	Plasma Control System .....	11
3.	Diagnostic Systems and Physics Potential.....	12
3.1.	Magnetic Diagnostic System .....	12
3.2.	Core Profile Diagnostics.....	13
3.2.1.	Thomson Scattering.....	13
3.2.2.	Charge-exchange spectroscopy (CER): impurity, main-ion .....	13
3.2.3.	Motional Stark Effect (MSE).....	14
3.2.4.	ECE systems .....	14
3.2.5.	Multichannel Interferometer .....	15
3.2.6.	Profile reflectometer for fast electron density profiles.....	15
3.3.	Survey Diagnostics.....	16
3.3.1.	Visible survey spectrometers (3).....	16
3.3.2.	Fast bolometer (1) .....	16
3.3.3.	Soft x-ray arrays (3).....	16
3.3.4.	Medium x-ray array (1) .....	16
3.3.5.	Hard x-ray scintillators (20).....	16
3.3.6.	Fast cameras (2) .....	16
3.4.	Turbulence Diagnostics.....	16
3.4.1.	Beam Emission Spectroscopy (BES) .....	16
3.4.2.	Phase Contrast Imaging (PCI).....	17
3.4.3.	Doppler backscattering (DBS) – density fluctuations (turbulence) and flow.....	18
3.4.4.	Correlation electron cyclotron emission (CECE) for turbulence and profiles.....	18
3.4.5.	Cross-polarization scattering (CPS) – internal magnetic fluctuations .....	19
3.4.6.	ECE IMAGING (ECEI) .....	19
3.4.7.	Faraday-effect Radial-Interferometer-Polarimeter (RIP).....	20
3.5.	Energetic Particle Diagnostics .....	21
3.5.1.	Fast Ion Deuterium Alpha Spectroscopy (FIDA) .....	21
3.5.1.1.	Fast Ion Deuterium Alpha Spectroscopy (S-FIDA) .....	21
3.5.1.2.	Fast Ion Deuterium Alpha Imaging (I-FIDA).....	22
3.5.2.	Fast Ion Loss Detector (FILD).....	22
3.5.3.	Neutron Rate Detectors.....	23
3.5.4.	Ion Cyclotron Emission (ICE) .....	24
3.5.5.	Imaging Neutral Particle Analyzers (INPA).....	24
3.5.6.	Gamma Ray Imager (GRI).....	24

3.5.7.	Outreach Ideas in EP physics.....	25
3.6.	Boundary Diagnostics .....	27
3.6.1.	Filterscopes .....	27
3.6.2.	Multichordal Divertor Spectrometer (MDS) .....	27
3.6.3.	Bolometer.....	27
3.6.4.	Divertor Thomson Scattering.....	27
	Fenton Glass (glassf@fusion.gat.com), GA.....	27
3.6.5.	Fast neutral pressure (ASDEX) gauges.....	29
3.6.6.	Coherence Imaging Spectroscopy (CIS) flow camera .....	29
3.6.7.	IR cameras .....	29
3.6.8.	Plunging probes (2) .....	30
3.6.9.	DiMES/MiMES.....	30
3.6.10.	Divertor EUV/VUV Survey Spectrometer (DivSPRED).....	30
3.6.11.	Penning & Baratron Gauges .....	30
3.6.12.	Fixed Langmuir probes.....	30
3.6.13.	DiMES TV (Visible filtered imaging).....	31
3.6.14.	Wide Spectral Emission (WiSE)Spectroscopy .....	31
3.6.15.	Fast Thermocouples.....	31
3.6.16.	Tangential TV .....	31
3.6.17.	LLAMA (Lyman-alpha measurement apparatus).....	31
3.6.18.	Tile Current Monitors.....	32
3.6.19.	Surface Eroding Thermocouples (SETCs).....	32
3.7.	General signal viewing.....	33
3.7.1.	Reviewplus.....	33
3.7.2.	OMFIT SCOPE module .....	33
3.7.3.	TRAVERSER .....	33
3.7.4.	pySpecview .....	33
3.8.	Equilibrium.....	33
3.8.1.	EFIT.....	34
3.9.	Profile fitting.....	34
3.9.1.	TANH .....	34
3.9.2.	ZIPFIT .....	34
3.9.3.	QUICKFIT.....	34
3.9.4.	OMFITprofiles.....	35
3.9.5.	Pyped toolkit .....	35
3.9.6.	GProfiles.....	35
3.9.7.	pyTomo.....	35
3.10.	Source deposition .....	35
3.10.1.	ONETWO and AutoONETWO .....	35
3.10.2.	TRANSP .....	35
3.11.	Integrated modeling tools .....	35
3.11.1.	OMFIT.....	35
3.11.1.1.	kineticEFITtime.....	36
3.11.1.2.	Boundary Toolbox.....	36
3.11.2.	efitviewer overlays .....	36
3.11.3.	pyped (Osborne tools) .....	36

4.	Planning Experiments .....	37
5.	Mini-proposal Template.....	38
6.	Acknowledgements.....	44

## 1. DIII-D Key Physics Parameters

R J Buttery ([buttery@fusion.gat.com](mailto:buttery@fusion.gat.com)), GA.

### Dimensional:

Major radius 1.7m, Minor Radius 0.6m,

Density typically  $0.3-1.5 \times 10^{20} \text{m}^{-3}$

Plasma current 0.4 to 2MA, Toroidal Field 0.6 to 2.17T

Safety factor at 95% surface  $\sim 2-12$

Heating power: 20MW beam (25MW planned), 3MW ECH (9MW planned), 1MW helicon

### Normalized:

Magnetic Reynolds number  $10^9$ ,  $\rho^* = .005-0.01$ ,  $v^* = 0.01-10$

$\beta$  to 5%,  $\beta_N$  to 5,  $\beta_P$  to 3, fast ion fraction from 0 to 40%,

$\beta_{FI} \leq \beta_{\text{thermal}}$ ,  $v_{\text{fast ion}} \sim v_{\text{Alfvén}}$ ,  $v_{\text{electron thermal}} \gg v_{\text{Alfvén}}$

## 2. DIII-D Facility Specifications

### 2.1. Tokamak Systems

R J Buttery ([buttery@fusion.gat.com](mailto:buttery@fusion.gat.com)), GA.

Plasma Current,  $I_p$ : up to 2MA, direction can be changed once per day between shots

Toroidal Field, BT: Up to 2.17 T on geometric axis, direction can be changed overnight

Shapes: Almost anything that will fit in the vessel due to advanced feedback shape control hardware/software system, vis. Inner wall limited, SN and DN diverted, indented bean shapes, both positive and negative triangularity, elongation up to 2.0, triangularity up to 0.8,

Pulse length: up to 10 sec

$n_e$ : up to  $1.5 \times 10^{20} \text{m}^{-3}$

$T_e$ : up to 15 keV on axis

$T_i$ : up to 15 keV on axis

Plasma Facing Components: carbon tiles, either ATJ or CFC

Primary Impurity: carbon

Material Exposure Systems: Divertor strike point exposure (DiMES), Outer midplane exposure (MiMES), retracable between shots, sample changes take  $\sim 30$  min

#### 2.1.1. Non-axisymmetric magnetic perturbations

Carlos Paz Soldan ([pazsoldan@fusion.gat.com](mailto:pazsoldan@fusion.gat.com)), GA.

C-coils: 6 window-frame coils on outer midplane, 4 turns, up to 28 kAt

I-coils: 6 window-frame coils above the midplane, 6 coils below the midplane, single turn, up to 7 kAt

C P/s: 5 supplies, single polarity, up to 7 kA, up to 280 V, minimum rise

time 20 ms

SPAs: 4 supplies, bipolar, up to 4.3 kA, up to 450 V, minimum rise time  
1 ms, maximum modulation frequency up to 2 kHz

Super-SPAs: 6 modules, bipolar, up to 2.7 kA (combinable x3 up to 7 kA), up to 300 V,  
minimum rise time 1 ms, maximum modulation frequency up to 4 kHz

Audio Amps: 24 modules, bipolar, up to 0.2 kA (combinable x6 up to 1.2 kA), up to 100  
V, minimum, rise time sub-ms, maximum modulation frequency 40 kHz

## 2.2. Heating, Fueling and Control Systems:

DIII-D presently has three heating and current drive systems: neutral particle beam injection, electron cyclotron resonant heating, and new helicon ultra-high harmonic fast wave RF system. It also has a fast wave antenna and infrastructure, though mothballed at present.

### 2.2.1. Neutral Beam Injection Systems:

Tim Scoville ([scoville@fusion.gat.com](mailto:scoville@fusion.gat.com)), GA.

Neutral beams are the present main workhorse for plasma heating and current drive. DIII-D has a highly flexible neutral beam system with four fixed on-axis co-injected beams (or counter if plasma current reverse), two variable on/off axis co-injected beams, and two fixed off axis toroidally steerable beams. Beam energy and power can also be controlled in real time, enabling decoupling of momentum and power, and control over energetic ion effects.

Specifications: 4 beamlines, 2 positive-ion sources per beamline

Pinj: up to 20 MW

Fuel: D<sub>2</sub>, H<sub>2</sub>, He

Energies: up to 93 kV, typical operating range 45 – 85 kV, power ratios at 81 kV:

Full energy 76%, Half energy 17%, Third energy 7%

Pulse Length: Up to 3.5 sec at 81 keV, longer at lower energies

Modulation: up to 2ms on/8ms off for hundreds of cycles during a shot

Aiming/deposition (on- or off-axis, co- or counter-injection): 10 MW fixed on-axis injection at the midplane in the co-injection direction. 5 MW variable off-axis power from 0° to 16.4° from the horizontal in the co-injection direction. 5 MW fixed off-axis power at 18.4° from the horizontal in either the co-injection or counter-injection direction.

Aiming/deposition (co- or counter-injection):

15 MW co-injection (in the same direction as the usual plasma current) with 10MW of this on axis and 5MW variable off-axis.

5 MW (fixed off axis) co-injection or counter-injection (opposite the usual plasma current direction).

Density limits (lower – shinethrough): dependent on plasma shape, beam power, etc. – limited by a pyrometer interlocked on armor tile surface temperature < 800°C.

Variable Beam Energy: seven ion sources now capable of up to 20 kV energy change in 0.5 sec during plasma shot. Also capable of varying perveance in a shot, during which beam current can be changed by up to 30% at fixed beam energy.

Low voltage beams: With special preparations, some beams can be run at very low voltages in the 15-20 kV range.

Feedback control: Plasma Control System provides simultaneous control of injected beam power and applied torque

### 2.2.2. ECH Systems: 2016 - 6 gyrotrons , 2017 up to 7 gyrotrons

John Lohr ([lohr@fusion.gat.com](mailto:lohr@fusion.gat.com)), GA.

ECH on DIII-D provides multiple useful applications. Principally these include:

- Electron heating to reach more reactor-relevant transport regimes, and to preheat plasmas early in the discharge to slow and control current profile evolution
- Highly localized perturbative capabilities with precise deposition spatially and in time, which is very valuable to study transport physics
- Opportunity to switch between pure heating and current drive
- Localized current drive is effective for controlling the modes, and can even be target into the center of magnetic islands, causing them to close
- Current drive can also be driven off axis, and with multiple gyrotrons, and this can be used to precisely tune the current profile to make high stability limit steady state discharges

Its principle limitations are (i) a density cut off which limits access by EC at high density, can lead to refraction of the EC beam about the vessel (with risk to diagnostic damage), and (ii) a decrease in current drive when deposited far off axis or in cold plasmas.

Key parameters:

$P_{ECH}$ : > 4 MW injected 2020, up from 3.6 MW in 2017 campaign

Wave modes: Arbitrary elliptical polarization, frequency 110 GHz and 117.5 GHz

Pulse Length: Typically up to 5 sec into tokamak but gyrotrons tested to 10 sec. at CPI, 8 sec at GA—pulse length maximum limited administratively due to transmission line limits and gyrotron cyclic thermal fatigue

Modulation: Up to 5 kHz with sinusoidal waveform, about 2 kHz with rectangular waveform

RF Aiming / Deposition: capable of real time or rapid pre-programmed steering in both toroidal ( $\pm 20$  degrees about the perpendicular), and poloidal (over  $40^\circ$ ) directions  $40^\circ/\text{sec}$  each direction.

Plasma density limit due to refraction – dependent on density profile, magnetic field and details of aiming, eg. Maximum of line average density  $\sim 7 \times 10^{19}$ , (peak value higher) at 2.1T magnetic field on axis.

Just commissioned in 2020, is a new single line top launch system, which was demonstrated to lead to approximately double the current drive compare to traditional outline launch (Chen APS 2019 post deadline invited talk).

### 2.2.3. Helicon Ultra High Harmonic Fast Wave

Andrea Garofalo ([garofalo@fusion.gat.com](mailto:garofalo@fusion.gat.com)), Bob Pinsker ([pinsker@fusion.gat.com](mailto:pinsker@fusion.gat.com)), GA.

A new traveling wave antenna coupled to a 1MW Klystron is being installed in 2020 to test potential for efficient current drive on DIII-D and robust coupling. The goal is to demonstrate this as a viable techniques for future fusion reactors, and also as a highly enabling tool for DIII\_D advance tokamak research.

For DIII-D, the principal benefits are:

- Significantly extra off axis current drive power to raise ideal MHD beta limits and improve transport properties
- This also affords the opportunity to drive current without torque, to evaluate AT scenarios with more reactor-relevant transport properties.
- This also provides current drive at higher densities than ECH (ECH being subject to cut-off), and thus will be helpful in exploring AT plasmas at higher particle and energy densities, for more reactor relevant core parameters and with more radiative mantle and dissipative divertors.

The parameters for the 2020 system are:

Source power of up to 1.2 MW at 476 MHz

Coupled power level depends on the SOL density profiles, expected to be more than 0.75 MW to the plasma core at parallel index of refraction  $n_{||}=3$  with a high toroidal directivity, either co-current or counter-current drive selectable between discharges

Wave mode: fast wave in the lower hybrid range of frequencies ("helicon")

Antenna: 30-element toroidal array of antenna modules, 1.5 m wide, operated as a traveling wave antenna of the 'comb-line' type, mounted in the vessel above the midplane

Pulse length: up to 5 sec (CW source, pulse length set by antenna cooling)

### 2.2.4. High Field Side Lower Hybrid Current Drive

Steve Wukitch ([wukitch@psfc.mit.edu](mailto:wukitch@psfc.mit.edu)), MIT.

This system is presently being designed and constructed for installation in 2021.

## 2.3. Pellet / Gas Systems

DIII-D has an extremely flexible array of particle, fueling and gas control systems:

### 2.3.1. Gas Injection

Patrick Byrne ([byrnep@fusion.gat.com](mailto:byrnep@fusion.gat.com)), GA.

Fast Gas Injection Locations: 45 deg above outer midplane, bottom lower outer shelf surface

Slow gas Injection Locations: Outer midplane, top under upper out baffle, top upper inner baffle surface, small angle slot divertor surface, bottom in private flux region, bottom under lower outer shelf.

Recently upgraded to an FPGA based control system - Full uptime for all 12 piezo valves. Expect improvements in uptime, valve availability and signal/noise ratio, reductions in manpower & pit time requirements, as well as faster valve response time - expect response time will be conductance limited by injection lines.

Flow rates: 1-180 Torr-L/s  
Fast gas valve response time: 5ms  
Slow gas valve response time: 200ms  
Standard gas species: D, H, He, N, Ne, Ar.  
Limited availability: Xe, Kr, CD<sub>4</sub>, CH<sub>4</sub>, 13CD<sub>4</sub>, mixtures

### 2.3.2. Vacuum and Wall Conditioning

Chris Chrobak ([chrobak@fusion.gat.com](mailto:chrobak@fusion.gat.com)), GA.

DIII-D is equipped with systems that provide excellent control of density and machine conditions:

- Axisymmetric cryogenic pumping from bottom (below lower outer shelf), and top (behind upper inner and upper outer baffles).
- Argon frosting capability for Helium cryo-sorption pumping
- Helium glow discharge wall conditioning between shots
- Periodic vessel baking to 350C and boronization
- Newly commissioned in 2019 is real time wall conditioning through pellet injection (see section 2.3.6).

### 2.3.3. Deuterium Pellet Injection:

Daisuke Shiraki ([shirakid@fusion.gat.com](mailto:shirakid@fusion.gat.com)), ORNL.

Pellet fueling and ELM pacing – 3 injectors:

Deuterium Fueling Pellets: cylindrical, 0.9mm diameter, particles/pellet, up to 20 Hz/injector, Locations: outer midplane, top, HFS inside wall at 45 degrees, below the midplane toward the lower X-point

### 2.3.4. Laser Blow Off

Nathan Howard ([nthoward@psfc.mit.edu](mailto:nthoward@psfc.mit.edu)), Tom Odstrcil ([odstrcilt@fusion.gat.com](mailto:odstrcilt@fusion.gat.com)) GA

A new laser blow-off (LBO) diagnostic installed at port 105° R+1 of DIII-D tokamak enables studies of both impurity and electron heat transport. Utilizing high energy (up to 1.2J), pulsed (up to 50Hz) Nd:YAG laser and fast, piezo-electric steering optics, this new system is capable of introducing multiple, impurity injections into a single DIII-D plasma discharge with precise timing. Control of the laser energy combined with remote control of the beam size and focus allow for an arbitrary selection of both the energy density incident on coated target films and the number of ablated particles. These capabilities provide a means for efficient introduction of a wide range of target materials (Li to W) into DIII-D plasmas, enabling the study of trace, non-intrinsic, low and high-Z impurity transport. Alternatively, the system can also introduce larger, perturbing amounts of impurities that can be used for cold pulse propagation studies and validation of atomic physics data.

Nd:YAG laser runs with 10Hz repetition rate, therefore the time of the first injection can be selected arbitrarily, but the other injection must follow in times which are a multiple of 100ms from the first one. The size of the ablation spot can be changed continuously up to 5mm in diameter. However, the amount of the impurity which after ablation reach the plasma core depends on the edge and SOL screening. Best penetration is usually in L-mode and QH-mode, while the

worst is in H-mode with high gas puff and electron heating. Therefore an **optimization of ablation spot size is necessary** before the experiment.

#### 2.3.5. Impurity Granule Injector (IGI):

Alessandro Bortolon ([abortolon@pppl.gov](mailto:abortolon@pppl.gov)), PPPL.

Injection of Li, B, C, Si granules, range of sizes from 0.3 – 0.9 mm

Injection frequency up to 500 Hz (average, for small granules)

Injection speed: 50-150 m/s

Location: outer midplane horizontal launch.

#### 2.3.6. Impurity Powder Dropper (IPD):

Alessandro Bortolon ([abortolon@pppl.gov](mailto:abortolon@pppl.gov)), PPPL.

Gravitational injection of impurities in powder, with particle size 5-100 microns.

Materials: Li, B, BN (tested on DIII-D); B<sub>4</sub>C, C, Sn (tested on the bench). Use of some materials (e.g. Li) requires special approval.

Three independent feeders with dedicated reservoirs allow using more of one material in the same experiment.

Location: R=1.5 m at 195 degrees, through SAS.

Supports research in: real-time wall conditioning, pedestal and ELM control, enhanced divertor dissipation with low-Z/non-recycling, dust effects.

#### 2.3.7. Impurity Single Granule Dropper:

Alessandro Bortolon ([abortolon@pppl.gov](mailto:abortolon@pppl.gov)), PPPL.

Timed, gravitational injection of impurities in form of single granules

Particle size 50-800 microns.

Materials: Li, C, Al, Si.

Location: R=1.5 m at 195 degrees, through SAS (replaces a powder feeder in IPD).

Goal: non-perturbative study of impurity transport in the SOL.

#### 2.3.8. Massive Gas Injection:

Daisuke Shiraki ([shirakid@fusion.gat.com](mailto:shirakid@fusion.gat.com))

Massive Gas Injection: two systems, Locations: above and below outer midplane, Species: D, H, Ne, Ar, large quantities only (> 50 torr-L)

This system is typically used for disruption mitigation.

#### 2.3.9. Shattered Pellet Injection:

Daisuke Shiraki ([shirakid@fusion.gat.com](mailto:shirakid@fusion.gat.com)), ORNL.

Shattered Pellet Injection: 2 systems, cryogenic pellets shattered in injection guide tube to produce spray of micro-shards, Location: above the midplane at two toroidal locations 135° apart. D Ne Ar pellets. Large quantities only (>100 torr-L)

This system is typically used for disruption mitigation.

#### 2.3.10. Solid Argon pellet injector

Daisuke Shiraki ([shirakid@fusion.gat.com](mailto:shirakid@fusion.gat.com)), ORNL.

Solid Argon pellet injector: above midplane, small (10-16 Torr-L) cryogenic Ar pellets

This system is typically used for disruption mitigation, or initiation for studies of mitigation.

#### 2.3.11. Shell pellet injector

Nick Eidietis ([Eidietis@fusion.gat.com](mailto:Eidietis@fusion.gat.com)), GA

DIII-D has recently implemented a injector capable of injecting shell pellets containing powder. This enables a payload to be delivered to the plasma core, and thus quench the disruption from the inside out - greatly improving assimilation of quench species and facilitating dissipation of current and runaway electrons (see IAEA FEC 2018, Eidietis).

This system consists of a pneumatic injector for thin shell (plastic or diamond) pellets containing a powder payload in order to study core impurity deposition for disruption mitigation. Location: LFS midplane, 120° toroidal angle, horizontal launch. Typical pellets are 3.6mm diameter, 40um thick diamond pellets with boron fill, although pellets up to 1cm diameter can be accommodated.

References: 1. E.M. Hollmann et al, PRL 122, 065001 (2019). 2. Eidietis IAEA FEC 2018

#### 2.4. Plasma Control System

Al Hyatt ([hyatt@fusion.gat.com](mailto:hyatt@fusion.gat.com)), GA.

Shape control – Digital; real-time equilibrium reconstruction, multipoint (up to 15) shape locations plus X-point and/or Strike Point divertor control

Feedback systems – many plasma parameters are measured and can be feedback controlled by selected actuators. Examples are stored energy, local toroidal rotation, line average density, local density, divertor radiated power

Feedback physics actuators – input NBI power, input NBI torque, input NBI voltage, input ECH power, input ECH local current drive, deuterium gas fueling, loop voltage, impurity gas injection, 3D magnetic perturbations

### 3. Diagnostic Systems and Physics Potential

See this link for latest details: <https://diii-d.gat.com/diii-d/DiagInfo>

#### 3.1. Magnetic Diagnostic System

L. Bardoczi ([bardoczil@fusion.gat.com](mailto:bardoczil@fusion.gat.com)) and E. Strait ([strait@fusion.gat.com](mailto:strait@fusion.gat.com)), GA

**What is measured:** Magnetic field outside the plasma, at the vacuum vessel wall.

Quantity Measured	Range of Measurement	Region	Spatial Resolution	Time Resolution
Axisymmetric poloidal flux	$\Phi < 20$ Weber	44 loops spaced poloidally	$\Delta\theta \sim 15^\circ$	500 $\mu$ s
Diamagnetic toroidal flux	$\Phi_D < 0.1$ Weber	Average over poloidal cross-section		500 $\mu$ s
Toroidal field	$B_t < 4$ T	4 loops, outboard side	$\Delta\phi \sim 90^\circ$	500 $\mu$ s
Total poloidal field (tangential to wall)	$B_p < 2$ T	90 loops spaced poloidally & toroidally	$\Delta\phi \sim 30-180^\circ$ $\Delta\theta \sim 15^\circ$	500 $\mu$ s
Total radial field (normal to wall)	$B_r < 0.2$ T	50 loops spaced poloidally & toroidally	$\Delta\phi \sim 30-90^\circ$ $\Delta\theta \sim 30^\circ$	500 $\mu$ s
Non-axisymmetric poloidal, radial field	$\Delta B_p, \Delta B_r \sim 0.1-50$ mT	120 differential pairs	$\Delta\phi \sim 30-45^\circ$ $\Delta\theta \sim 10-40^\circ$	20 $\mu$ s
Poloidal field fluctuations (dBp/dt)	$\delta B_p \sim .004-4$ mT @50 kHz	70 loops: poloidal array & outboard side toroidal array	$\Delta\phi \sim 5-30^\circ$ $\Delta\theta \sim 15^\circ$	2 $\mu$ s
Poloidal field fluctuations (dBp/dt)	$\delta B_p \sim .004-4$ mT @15 kHz	7 loops: inboard side toroidal array	$\Delta\phi \sim 5-30^\circ$	2 $\mu$ s
High-frequency poloidal field fluctuations (dBp/dt)	$\delta B_p \sim 0.1-100$ $\mu$ T @1 MHz	5 loops: compact array on the outboard side	$\Delta\phi \sim 2-15^\circ$ $\Delta\theta \sim 7^\circ$ $\Delta r \sim 5$ cm	0.5 $\mu$ s
Plasma current	$I \sim 10^6$ A	3 Rogowski loops spaced toroidally		500 $\mu$ s
Coil current		40+ Rogowski loops on coil leads		500 $\mu$ s

#### Typical applications:

Axisymmetric poloidal flux: Equilibrium reconstruction, real-time control of plasma shape and position

Diamagnetic flux: Plasma kinetic energy

Toroidal field: Main field for plasma confinement and stability

Total poloidal field: Equilibrium reconstruction, real-time control of plasma shape and position

Total radial field: Secondary data for equilibrium reconstruction and non-axisymmetric fields

Non-axisymmetric poloidal, radial field: Field errors, growing or saturated instabilities without rotation ( $\omega_{\text{real}} \sim 0$ ), response of stable plasma modes to applied non-axisymmetric fields, damping rate of marginally stable modes. (Typical values of  $\delta B_p/B_p$ :  $10^{-4} \sim 10^{-2}$ .)

Poloidal field fluctuations: growing or saturated instabilities with rotation ( $\omega_{\text{real}} \neq 0$ ), **rapidly growing instabilities with  $\omega_{\text{real}} \neq 0$**

High-frequency poloidal field fluctuations: short wavelength and/or rapidly rotating instabilities

## 3.2. Core Profile Diagnostics

### 3.2.1. Thomson Scattering

Fenton Glass ([glassf@fusion.gat.com](mailto:glassf@fusion.gat.com)), GA.

The DIII-D Thomson scattering system measures the electron temperature and density along a laser beam path. There are four beam paths: a vertical path at  $R = 1.94\text{m}$  measures 44 spatial locations from the center of the plasma to the top of the vessel at 230 pulses per second using 7 lasers; a horizontal path measures 10 spatial locations near the center of the vessel at 40 pulses per second using 2 lasers; and a second vertical path at  $R = 1.485\text{m}$  measures up to 16 spatial locations, split between the lower and upper divertor regions of the vessel at 50 pulses per second using 1 laser. A third vertical path at  $R = 1.335\text{m}$  is accessible by re-directing the  $R = 1.485\text{m}$  beam path to measure 12 spatial locations in the lower divertor at 50 pulses per second, using the same laser. The temperature measurement range is 0.2 to 5000 eV for densities above  $5 \times 10^{18} \text{ m}^{-3}$  with an error of roughly 5-10%, depending on conditions. The spatial resolution is typically 1-2 cm, but the upper edge region of the plasma has 0.5 cm resolution to resolve the steep gradients of H-mode plasmas. This higher spatial resolution region on the  $R = 1.94\text{m}$  vertical beam path can be lowered up to  $\sim 13.5\text{cm}$  to better match various plasma gradient locations.

### 3.2.2. Charge-exchange spectroscopy (CER): impurity, main-ion.

Impurity: Colin Chrystal ([Chrystal@fusion.gat.com](mailto:Chrystal@fusion.gat.com)), GA.

Main ion: Shaun Haskey ([shaskey@pppl.gov](mailto:shaskey@pppl.gov)), PPPL.

The Charge Exchange Recombination Spectroscopy (CER) system is used to measure ion temperature, poloidal and toroidal rotation, and impurity density. These are determined from the Doppler broadening, Doppler shift, and total intensity of the spectroscopic line. In addition, by using the radial force balance equation, the radial electric field in the plasma can be determined from these quantities.

The desired signal for the spectroscopic measurement is produced by charge exchange between neutrals in the neutral beams and ions in the plasma. For the impurity system typically we use lines radiated by charge exchange with fully stripped ions of low  $Z$  impurities (e.g. carbon, boron), since they exist everywhere in the discharge. For the “main-ion” system, the measurements are based on the deuterium or hydrogen ions directly. The measurement is spatially localized at the point where the viewchord crosses the neutral beam. The system can measure spectral lines in the wavelength range from 300 nm to 800 nm; the best sensitivity is in the visible and near IR from 400 to 800 nm.

The impurity system has 76 spatial views, 44 viewing tangentially, and 32 viewing vertically. The main-ion system has 32 tangential views. The views intersect the neutral beams at the midplane and span from approximately 1.28 to 2.32 m in major radius.

- Ion Temperature (Ti) from  $\sim 100 \text{ eV}$  to  $\sim 20 \text{ keV}$

- Toroidal and poloidal velocity from  $\sim 1$  km/s to  $\sim 500$  km/s
- Radius from 1.28 – 2.32 m covering with 20 views inside the magnetic axis, 88 views outside the magnetic axis with high resolution near the plasma boundary outside the magnetic axis
- Measurement period as low as 0.2 ms but typically 5.0 ms
- Workhorse diagnostic for radial profiles of ion temperature, rotation, impurity density, and radial electric field.

In addition to the above it is possible to use “main-ion” system to provide the following measurements

- Radial profiles of the isotope fraction (i.e.  $n_{H^+}/(n_{H^+} + n_{D^+})$ ) in mixed isotope plasmas
- Spectrally resolved measurements of the passive Balmer- $\alpha$  emission. This is similar to a filterscope, but spectrally resolved to provide details of the energy distribution of the neutrals
- Neutral beam velocity and emission brightness measurements: full, half, third energies
- Measurements of  $|B|$  based on stark splitting of the beam emission (MSE-LS)

### 3.2.3. Motional Stark Effect (MSE)

Brian Victor ([victorb@fusion.gat.com](mailto:victorb@fusion.gat.com)), Chris Holcomb ([holcomb@fusion.gat.com](mailto:holcomb@fusion.gat.com)), LLNL.

The motional Stark Effect (MSE) diagnostic measures the polarization angle of light emitted by neutral beam particles entering the plasma. From the polarization angle, the magnetic field pitch angle of the plasma can be found. These measurements are used as a constraint in our equilibrium solver, EFIT. MSE measurements are the primary constraint on the  $q$  profile inside the plasma.

There are three discrete MSE views of neutral beam emission from the 30L beam line. Each view measures the polarization angle near the midplane,  $Z = 0$ , of the tokamak. The ‘core system’ has 15 channels ranging between  $R = 1.53 - 2.25$  m. This view spans the magnetic axis of typical DIII-D plasmas and is the only view routinely used in equilibrium reconstructions. The ‘radial system’ has 10 channels between  $R = 1.67 - 2.09$  m. The ‘edge system’ has 15 channels between  $R = 1.99 - 2.27$  m with high spatial resolution in the pedestal region of the plasma. Measurements are localized to the intercept of the view with the neutral beam.

MSE data is used in the PCS system as constraints for real-time EFITs. Raw signals are sent to lock-in amplifiers and the outputs are digitized at 4 kHz. In addition, there is the capability to digitize the raw signals at 1 MHz.

Work is ongoing at DIII-D to implement an imaging MSE diagnostic. Multiple systems have been tested and the data implemented into equilibrium reconstructions. Imaging MSE systems have higher spatial resolution (limited by the view intercept with the neutral beam, not the channel-to-channel spacing), but lower temporal resolution ( $\sim 10$  Hz).

### 3.2.4. ECE systems

Max Austin ([austin@fusion.gat.com](mailto:austin@fusion.gat.com)), U Texas.

- Measure Electron Cyclotron Emission (ECE) from DIII-D plasmas.
- At typical DIII-D field strengths, ECE is in the microwave range, nominally 60-600 GHz.

- For part of that frequency range, the electron temperature  $T_e$  can be inferred directly from the power emitted at those frequencies.
- $T_e$  range: 10 eV to 20 keV.
- $T_e$  region: major radius  $150 \text{ cm} < R_{\text{maj}} < 230 \text{ cm}$  at mid-plane, usually covers entire plasma minor radius.
- $T_e$  resolution: 40 locations simultaneously with a spatial resolution of 2 cm and a time resolution of 2 microseconds.
- Applications:  $T_e(r,t)$  to measure heating effectiveness, plasma energy loss, flux surface oscillations, etc.

### 3.2.5. Multichannel Interferometer

Mike Van Zeeland ([vanzeeland@fusion.gat.com](mailto:vanzeeland@fusion.gat.com)), GA.

Beginning in 2004, the CO<sub>2</sub> interferometer on DIII-D was upgraded to an all-digital phase demodulation system. The new system is superior in terms of reliability, reduced noise, and increased bandwidth. All four chords are routinely digitized for 9 seconds of each discharge at a rate of 1.67 MS/s. This long digitization record, increased bandwidth, and reduced noise have significantly extended the scope of the interferometer to include far more than just feedback control of the density. The system is now able to track massive gas puff and pellet injection as well as both broadband and coherent fluctuations with  $dnL/nL$  as low as  $10^{-5}$  and frequencies up to 800 kHz.

#### Layout on DIII-D

There are a total of four interferometer chords that function on a routine basis; three vertical (V1, V2, V3) and one radial (R0). Toroidally, V1, V2, and V3 are located at 240 degrees and R0 is located at 225 degrees.

The major radius of each chord ( $R_m$ ) is:

$$V1 R_m = 1.48 \text{ m},$$

$$V2 R_m = 1.94 \text{ m},$$

$$V3 R_m = 2.10 \text{ m}$$

### 3.2.6. Profile reflectometer for fast electron density profiles

Lei Zeng ([zeng@fusion.gat.com](mailto:zeng@fusion.gat.com)), Terry Rhodes ([trhodes@ucla.edu](mailto:trhodes@ucla.edu)), UCLA.

Measures electron density profiles  $n_e(r)$  with high time and space resolution (25  $\mu\text{s}$  and 1 cm).

Measurement Ranges Radial ranges from SOL to deep core,  $\rho \sim 0.2$  or smaller, depending on plasma parameters

Measurement region Density profiles are made along a major radius axis very close to the vacuum midplane.

Resolution  $dt \sim 25 \mu\text{s}$ ,  $dr \sim 1 \text{ cm}$

Special notes The profile system requires no neutral beams for operation and so can obtain data in a variety of plasmas – ohmic, L-mode, and H-mode.

Physics applications Used for fast dynamics of ELMs, L-H transitions, etc. as well as measurements of particle transport using modulation of gas puff, ECH, or RMP techniques.

### 3.3. Survey Diagnostics

#### 3.3.1. Visible survey spectrometers (3)

Eric Hollmann ([ehollmann@ucsd.edu](mailto:ehollmann@ucsd.edu)), UCSD.

Average speed (1 kHz) visible light (300 – 900 nm) low spectral resolution (~0.5 nm) survey spectra along single fiber-coupled view chords viewing across plasma.

#### 3.3.2. Fast bolometer (1)

Eric Hollmann ([ehollmann@ucsd.edu](mailto:ehollmann@ucsd.edu)), UCSD.

Medium fast (50 kHz) measurement of total radiated brightness (2 eV – 10 keV) on poloidal fan across plasma with 30 view chords.

#### 3.3.3. Soft x-ray arrays (3)

Eric Hollmann ([ehollmann@ucsd.edu](mailto:ehollmann@ucsd.edu)), UCSD.

Medium fast (50 kHz) measurement of soft x-ray (2 keV – 10 keV) brightness on 3 poloidal fans across plasma with 88 view chords.

#### 3.3.4. Medium x-ray array (1)

Eric Hollmann ([ehollmann@ucsd.edu](mailto:ehollmann@ucsd.edu)), UCSD.

Medium fast (50 kHz) measurement of mid x-ray (20 keV – 200 keV) brightness on 1 poloidal fan across plasma with 12 view chords.

#### 3.3.5. Hard x-ray scintillators (20)

Eric Hollmann ([ehollmann@ucsd.edu](mailto:ehollmann@ucsd.edu)), UCSD.

Medium fast (50 kHz) measurement of uncollimated hard x-ray flux (0.5 MeV – 50 MeV) at 20 locations outside vacuum vessel.

#### 3.3.6. Fast cameras (2)

Claudio Marini ([marinic@fusion.gat.com](mailto:marinic@fusion.gat.com)), Eric Hollmann ([ehollmann@ucsd.edu](mailto:ehollmann@ucsd.edu)), UCSD.

Medium fast (10 kHz) visible light (400 – 800 nm) imaging of plasma, typically used with inference filters (1-10 nm FWHM) to isolated specific spectral lines.

### 3.4. Turbulence Diagnostics

#### 3.4.1. Beam Emission Spectroscopy (BES)

G. McKee, [mckee@fusion.gat.com](mailto:mckee@fusion.gat.com); Z. Yan, [yanz@fusion.gat.com](mailto:yanz@fusion.gat.com)  
University of Wisconsin-Madison.

Beam Emission Spectroscopy (BES) is a multichannel diagnostic that measures long-wavelength (ion gyroradius-scale) density fluctuations that arise from a range of turbulence and other

instabilities that often arise in magnetically confined plasmas. The basic principle of BES is to measure optical emissions from neutral beams that are injected to heat, fuel and rotate plasmas. Specifically, the Balmer-alpha ( $n=3-2$ ,  $\lambda_0=652-655$  nm) emission from the collisional fluorescence of excited hydrogenic neutral beam atoms is measured with specialized high throughput optics and detectors. Cross-beam viewing geometry of the heating beam (emission source) and optical line-of-sight allow for good spatial resolution.

Basic parameters of the measurement are as follows:

- Measured quantity: Balmer-alpha light intensity emission (high time resolution)
- Physics quantity: plasma electron and ion density fluctuations:  $\tilde{n}/n$
- Number of channels: 64
- Radial range:  $0.25 < \rho$  (normalized minor radius)  $< \sim 1$ 
  - Along the outboard midplane at one toroidal location
- Configuration: the 64 channels can be arranged into multiple configurations that can be radially moved between shots, e.g.,:
  - Radial array of 64 channels (covering most of minor radius)
  - $32 \times 2$  array (wide radial coverage with limited poloidal resolution)
  - $8 \times 8$  array (turbulence imaging)
- Frequency: 1 MHz
- Duration: up to 8 sec., full discharge duration can be covered
- Measurement requirements: Injection of 150 neutral beam source (right or left)
- Derived turbulence parameters:
  - Frequency spectra
  - Radial correlation length
  - Poloidal correlation length
  - Decorrelation time
  - 2D  $S(k_r, k_\theta)$  wavenumber spectra
  - Poloidal velocity fluctuations (e.g., zonal flow, Geodesic Acoustic Modes)
  - 2D velocimetry: radial-poloidal velocity field of eddy structures
- Observable instabilities:
  - Low-wavenumber turbulence (ion temperature gradient, trapped electron mode, resistive ballooning mode)
  - Energetic particle-driven modes (toroidal Alfvén eigenmodes, RSAE, e-GAM)
  - Magnetohydrodynamic instabilities (neoclassical tearing modes, edge localized modes, sawteeth)

### 3.4.2. Phase Contrast Imaging (PCI)

Chris Rost ([rost@fusion.gat.com](mailto:rost@fusion.gat.com)), Alessandro Marinoni ([marinoni@fusiomn.gat.com](mailto:marinoni@fusiomn.gat.com)), MIT.

- Line-integrated electron density fluctuations measured over closely-spaced vertical chords, absolutely calibrated
- Response over range  $10 \text{ kHz} < f < 2 \text{ MHz}$  and  $1 < k < 30 \text{ cm}^{-1}$ , covering intermediate- $k$  turbulence (upper end of ion scale, low end of electron scale); measurement covers outer plasma with  $r/a > 0.4$
- Measurement based on laser scattering, so compatible with all plasma heating schemes and parameter ranges

- Observations typically dominated by edge turbulence, especially from regions of large velocity shear
- Additional channel monitors  $0 < k < 5 \text{ cm}^{-1}$ , observing peak ion scale turbulence and coherent MHD; cross-correlation with DIII-D interferometer to measure toroidal  $n$
- Studies focus on turbulence and transport in the outer plasma, especially in the H-mode edge

### 3.4.3. Doppler backscattering (DBS) – density fluctuations (turbulence) and flow

Rongjie Hong ([rohong@ucla.edu](mailto:rohong@ucla.edu)), UCLA, Terry Rhodes ([trhodes@ucla.edu](mailto:trhodes@ucla.edu)), UCLA

Measures local values of intermediate- $k$  density fluctuations (turbulence) and fluctuation flow velocity in poloidal direction. Poloidal flow velocity which is often dominated by the local  $E \times B$  velocity.

Measurement Ranges Wavenumber range  $k \sim 1 - 12 \text{ cm}^{-1}$  and normalize range  $k\rho_s = 0.5-6$ . Radial spatial resolution  $\sim 0.5 \text{ cm}$ .

Measurement region Radial range depends on plasma parameters and polarization chosen, typically upper pedestal to deep core. Vertical region is roughly  $-10 \text{ cm}$  below vacuum midplane to  $+25 \text{ cm}$  above.

Resolution  $dk \sim 1 \text{ cm}^{-1}$ ,  $dt \sim 1\mu\text{s}$ ,  $dr \sim 0.5 \text{ cm}$ ,  $dV \sim 20\%$

Special notes The DBS system requires no neutral beams for operation and so can obtain data in a variety of plasmas – ohmic, L-mode, and H-mode. There are two DBS systems on DIII-D located  $180^\circ$  toroidally apart. This has been used to diagnose long correlation length ( $m \sim 0$ ,  $n \sim 0$ ) zonal flow activity as well as EHO etc.

Physics applications The Doppler backscattering technique has been utilized to determine radial electric field, geodesic acoustic modes, zonal flows, and intermediate scale ( $k \sim 1-6 \text{ cm}^{-1}$ ) density turbulence levels [1–4]. Doppler frequency typically depends upon both the background  $E \cdot B$  velocity as well as the intrinsic propagation velocity of the fluctuations. It is often found (although not always) that the  $E \cdot B$  velocity dominates in which case the measurement is a good estimate of local radial electric field. In that case fluctuations in the electric field can also appear as fluctuations in the Doppler shift frequency.

### 3.4.4. Correlation electron cyclotron emission (CECE) for turbulence and profiles

Guiding Wang ([wanggd@ucla.edu](mailto:wanggd@ucla.edu)) UCLA, Terry Rhodes ([trhodes@ucla.edu](mailto:trhodes@ucla.edu)), UCLA

Measures electron temperature fluctuations (turbulence) as well as electron temperature profiles over a range of magnetic fields, 1.6-2.1 T. Measurements at up to eight simultaneous radial positions are available.

Measurement Ranges Wavenumber range  $k \leq 0.5 \text{ cm}^{-1}$  and normalize range  $k\rho_s = 0-0.3$ . Radial spatial resolution  $< 0.5 \text{ cm}$ .

Measurement region Radial range depends on plasma parameters and polarization chosen, typically from top of pedestal to deep core. Vertical region is roughly  $+7.6 \text{ cm}$  above the vacuum midplane.

Resolution  $dk_r \sim 0.1 \text{ cm}^{-1}$ ,  $dt \sim 100 \text{ ms}$  for turbulence, 1 ms or shorter for coherent modes,  $dr < 0.5 \text{ cm}$ ,  $d\tilde{T}_e \sim 0.2\%$

Special notes The CECE system requires no neutral beams for operation and so can obtain data in a variety of plasmas – ohmic, L-mode, and H-mode.

Physics applications Measurements of electron temperature turbulence related to ITG and TEM type instabilities. In addition, coherent fluctuations such as GAMs, NTMs, etc. are routinely made.

#### 3.4.5. Cross-polarization scattering (CPS) – internal magnetic fluctuations

Terry Rhodes ([trhodes@ucla.edu](mailto:trhodes@ucla.edu)), UCLA, Rongjie Hong ([rohong@ucla.edu](mailto:rohong@ucla.edu))

Measures local values of magnetic fluctuations (turbulence) at a range of wavenumbers and radial locations.

Measurement Ranges Wavenumber range  $k \sim 0.5 - 15 \text{ cm}^{-1}$  and normalize range  $k\rho_s = 0.25-7$ . Radial spatial resolution depends on scattering geometry, can be as small as  $\sim 1 \text{ cm}$ .

Measurement region Radial range depends on plasma parameters typically upper pedestal to deep core. Vertical region is roughly -10 cm below vacuum midplane to +25 cm above.

Resolution  $dk \sim 1 \text{ cm}^{-1}$ ,  $dt \sim 1\mu\text{s}$ ,  $dr \geq 1 \text{ cm}$

Special notes The CPS system requires no neutral beams for operation and so can obtain data in a variety of plasmas – ohmic, L-mode, and H-mode.

Physics applications

CPS measures local values of magnetic fluctuations over a range of wavenumbers applicable to MTMs, KBMs, EM ETG, etc.

#### 3.4.6. ECE IMAGING (ECEI)

Yilun Zhu ([amzhu@ucdavis.edu](mailto:amzhu@ucdavis.edu)), UC Davis.

Microwave imaging diagnostics on DIII-D (electron cyclotron emission imaging [ECEI] and microwave imaging reflectometry [MIR]) record electromagnetic spectra in the millimeter-wave regime along multiple lines of sight at MHz digitization rates.

- ECE-Imaging consists of two microwave detector arrays positioned at the 270 degree mid plane port.
- Each detector array has 20 antennas arranged vertically whose field of view are collimated along roughly parallel lines of sight.
- The field pattern is adjustable, but covers roughly 20-50 vertical cm.
- Each antenna is coupled to tunable heterodyne mixing circuitry to discriminate 8 frequency bands. The range of adjustment spans from approximately 75-140 GHz.
- Signals are digitized at 1 MHz to provide 320 channels recording microwave intensity.
- During typical operation on DIII-D, these channels produce a 2D cross-sectional image of fluctuating electron temperature.

The 12-antenna MIR array views the tokamak through the same port, but provides an

additional reference source and 4 quadrature mixing channels per antenna so that both amplitude and phase of microwave power, either passive radiation or reflected probe beam, are recorded on 48 channels at 1 MHz. The frequency range is currently limited to roughly 60-70 GHz. During typical operation on DIII-D, this diagnostic provides 2D images of fluctuating electron density.

#### 3.4.7. Faraday-effect Radial-Interferometer-Polarimeter (RIP)

Jie Chen ([chenjie@ucla.edu](mailto:chenjie@ucla.edu)), David Brower ([brower@ucla.edu](mailto:brower@ucla.edu)), UCLA

Faraday-effect Radial-Interferometer-Polarimeter (RIP) measures line-integrated Faraday rotation angle and electron density along 3 horizontal chords at  $Z=0$  and  $\pm 13.5$  cm ( $Z=0$  corresponds to DIII-D mid-plane). The system is sensitive to low- $k$  fluctuations ( $k_{\perp} < 1/\text{cm}$ ) and has 1 MHz bandwidth. The measurement provides absolute amplitude of radial magnetic and density fluctuations with high resolution ( $\sim 1$  Gauss/ $\sqrt{\text{kHz}}$  and  $\Delta n/n \sim 0.01\%$  respectively). The sampling time is adjustable and typically set to 0.3 to 5 seconds. Starting from FY22 campaign, RIP bandwidth will be upgraded to 5 MHz (nominal) and 30 MHz (maximum) for high frequency fluctuation measurement. RIP measurements also provide equilibrium information of internal radial magnetic field and electron density, which can be used to constrain magnetic equilibrium, calculate magnetic axis vertical position and estimate central current density etc.

### 3.5. Energetic Particle Diagnostics

#### 3.5.1. Fast Ion Deuterium Alpha Spectroscopy (FIDA)

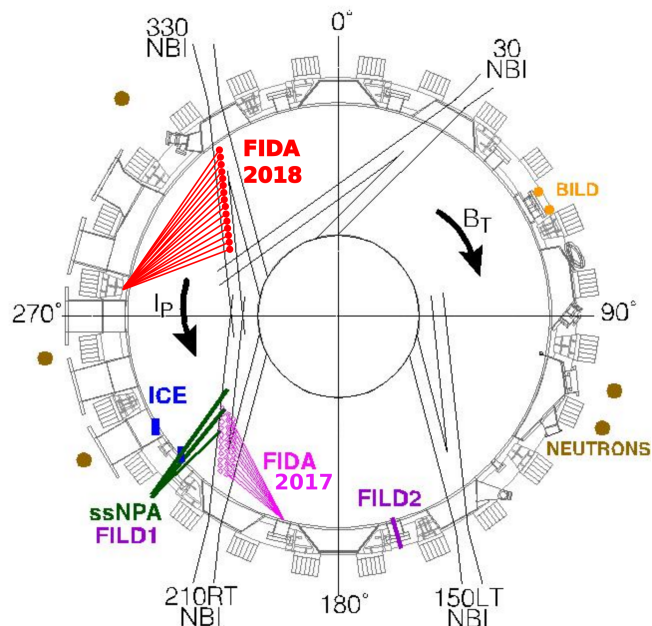


Figure 1. Topview of DIII-D fast ion diagnostics. “FIDA 2017” is obsolete. Both INPA1 and INPA2 view the 330 beamlines.

##### 3.5.1.1. Fast Ion Deuterium Alpha Spectroscopy (S-FIDA)

Deyong Liu ([liud@fusion.gat.com](mailto:liud@fusion.gat.com)), GA.

Bill Heidbrink ([heidbrink@fusion.gat.com](mailto:heidbrink@fusion.gat.com)), UC Irvine.

- **Measures** - Line integrated, Doppler-shifted Balmer- $\gamma$  light emission resulting from charge-exchange between fast ions and neutral particles. Centered at  $\lambda_0 = 656.1$  nm and sensitive to shifts up to  $\Delta\lambda_0 \sim 6$  nm.
- **Parameter Range**
  - Energy: detects light emission from 20-100 keV ( $\pm 15$  keV) ions
  - Pitch ( $v_{||}/v$ ): roughly  $0.5 \leq |v_{||}/v| \leq 1$
- **Resolution**
  - Spatial: 3 cm
  - Sampling Rate Spectral: typically 1kHz, up to 5 kHz
  - Sampling Rate bandpass PMT system: 1 MHz
  - Spectral: 0.7 nm
- **Region FIDA 2018**
  - 15 chords spanning R= 154-201 cm along 330LT beamline
  - Port location: 285R-1

The FIDA diagnostic is used to characterize fast-ion density profiles. FIDA is a version of charge-exchange spectroscopy and operates best with a source of neutrals, typically injected neutral beam particles, which are modulated to enable background subtraction. The fast-ion density is proportional to the intensity of the emission, while the shape of the

emitted spectrum contains information about the velocity distribution function. Multiple lines of sight at different radii can be used to obtain radial profile information. Synthetic diagnostic signals can be obtained through TRANSP/FIDASIM codes.

Currently only lines of sight on beam 330LT are used (FIDA 2018 in the figure).

*Provided by General Atomics.*

### 3.5.1.2. Fast Ion Deuterium Alpha Imaging (I-FIDA)

Deyong Liu ([liud@fusion.gat.com](mailto:liud@fusion.gat.com)), GA.

Bill Heidbrink ([heidbrink@fusion.gat.com](mailto:heidbrink@fusion.gat.com)), UC Irvine.

- Measures: 2D image of the Doppler-shifted Balmer- $\alpha$  light emission resulting from charge-exchange between fast ions and neutral particles in the spectral region centered at  $\lambda_{\text{passband}} = 651.55$  nm and characterized by a width of  $\Delta\lambda \sim 1.5$  nm.
- Parameter Range
  - Energy: detects light emission from 20-100 keV ( $\pm 15$  keV) ions
  - Pitch( $v_{||}/v$ ): from +0.5 to +1
- Resolution
  - Spatial: < 2 mm
  - Sampling Rate: up to 200 Hz
  - Spectral: no spectral resolution, light integrated in the spectral region of width  $\Delta\lambda \sim 1.5$  nm centered at  $\lambda_{\text{passband}} = 651.55$  nm.
- Region
  - Field of view spanning R= 150-205 cm, focused on the 330LT beamline
  - Port location: 285R-1

The I-FIDA diagnostic is used to characterize fast-ion density profiles with higher accuracy than the spectroscopic FIDA, thanks to a much higher spatial resolution and no cross-channel uncertainty in the absolute calibration. The diagnostic is also able to detect the redistribution of fast ions due to the interaction with MHD modes.

The lack in spectral resolution prevents reconstruction of the fast ion velocity distribution, but it is envisioned to combine I-FIDA measurements, to be used as constraints, with S-FIDA and INPA data to improve the velocity space reconstruction of these diagnostics.

I-FIDA is an active diagnostic that relies on modulation of the 330 LT beam to extract the active component of the signal from the measurements, by means of a background subtraction technique.

The codes TRANSP and FIDASIM are used for data interpretation.

*Provided by General Atomics with assistance from UC Irvine.*

### 3.5.2. Fast Ion Loss Detector (FILD)

Kenny Gage ([gagek@uci.edu](mailto:gagek@uci.edu)), Bill Heidbrink ([heidbrink@fusion.gat.com](mailto:heidbrink@fusion.gat.com)), UC Irvine.

- Measures- Energetic ions that reach scintillator based particle detectors located at the vessel wall.
- Parameter Range
  - Energy: detects 35-80 keV ions
  - Pitch( $v_{||}/v$ ): 0.09 ( $\pm .07$ ) to 0.82 ( $\pm .04$ )

- Resolution
  - Sampling Rate: 1 MHz (PMT), 160 Hz (CCD camera)
  - Spatial: Detects ions with gyroradii=1.5-8.5 cm  $\pm$ 1.3 cm
- Region
  - Port location: FILD1 is at 225°R-1 (45° below outer midplane), FILD2 is at 165°R0 (at the midplane)

The FILD diagnostic resolves ion energy and pitch information by using a CCD camera that records images of the scintillator surface, while the net signal is recorded with a multi-channel photomultiplier (PMT) with high time resolution. The detector orientation requires normal directions of magnetic field (negative values) and plasma current (positive values). Synthetic ion orbit modeling is available to investigate loss origins and orbit classification for a given plasma magnetic equilibrium.

*Provided by UC Irvine.*

### 3.5.3. Neutron Rate Detectors

Bill Heidbrink ([heidbrink@fusion.gat.com](mailto:heidbrink@fusion.gat.com)), UC Irvine; Deyong Liu ([liud@fusion.gat.com](mailto:liud@fusion.gat.com)), GA

- Measures - 2.5 MeV neutrons produced by D-D fusion reactions are detected using scintillators with photomultipliers (PMT), or moderated and detected using epithermal counters.
- Parameter Range
  - $10^9$  to  $10^{17}$  neutrons/sec
- Resolution
  - Sampling Rate: 50 kHz (scintillators), 1kHz (counters)
  - Spatial: volume averaged
- Region
  - Port location: plastic & ZnS scintillators with adjustable gain at 105° R+1; fixed gain scintillators at various locations; counters on the midplane near 255°.

The neutron emission rate is used as a volumetric proxy for the total number of high-energy fast ions. The absolutely calibrated measurement is obtained from combined output from several neutron counters (BF3, He3, and fission detectors) and fixed-HV scintillators. The counters provide the most stable absolute calibration, and the scintillators have superior time resolution. The scintillator detectors are useful when the source exceeds  $10^{11}$  neutrons/s but can be susceptible to x-ray contamination for electron density  $n_e < 5 \times 10^{18} \text{ m}^{-3}$ . Comparison of the adjustable plastic and ZnS signals are used to identify x-ray contamination in the scintillator signals or to measure hard x-rays in runaway electron experiments. There is also a BC412 scintillator with enhanced sensitivity to gammas from lower-energy runaways.

Synthetic neutron signals can be obtained through TRANSP/FIDASIM codes.

*Provided by UC Irvine with assistance from GA and Palomar Scientific.*

#### 3.5.4. Ion Cyclotron Emission (ICE)

Genevieve DeGrandchamp ([degrandchampg@fusion.gat.com](mailto:degrandchampg@fusion.gat.com)), Bill Heidbrink ([heidbrink@fusion.gat.com](mailto:heidbrink@fusion.gat.com)), UC Irvine.

- Measures- RF emission from ion cyclotron motion via loop antennas and old ICRH antenna straps at the wall.
- Resolution
  - Sampling Rate: 200 MHz for 5 seconds.
- Region
  - Toroidal tiles located at R = 242 cm at 232.5°, 247.5°, 262°, and 277.5° near the midplane
  - FW straps at R = 242 cm at 175° and 185°, centered about midplane
  - Poloidal tile at R = 242 cm at 247.5°, near the midplane
  - Centerpost tiles located near 255 and 260, near midplane

Ion cyclotron emission is created mainly by fusion products or by fast ions energized by kinetic instabilities. ICE is a relatively under-utilized diagnostic on DIII-D. Bursting ICE emission has been observed at primary and harmonic cyclotron frequencies during the excitation of fishbone modes. It is thought that the fishbones expel fast ions, which then excite magnetoacoustic waves through the anisotropic 'bump-on-tail' distribution function caused by the losses. The ICE diagnostic is also used to look at instabilities in connection with runaway electrons and parametric decay instabilities driven by the helicon antenna.

*Provided by UC Irvine.*

#### 3.5.5. Imaging Neutral Particle Analyzers (INPA)

Xiaodi Du ([duxiaodi@fusion.gat.com](mailto:duxiaodi@fusion.gat.com)), GA; Javi Gonzalez Martin ([javig14@uci.edu](mailto:javig14@uci.edu)), UCI

- Measures- Fast ions that charge exchange with either injected neutrals (aka "active charge exchange") or cold edge neutrals (aka "passive charge exchange") on a 2D image. One dimension corresponds with energy; the other with major radius across the plasma.
- Resolution
  - < 10 keV in energy, a few centimeters in radius. INPA1 measures co-passing ions along a narrow line in pitch. INPA2 measures trapped ions. The present temporal resolution is determined by the camera and is slower than 1 ms but work is underway to split the signal to measure fluctuations with <200kHz bandwidth.

For more information consult Nuclear Fusion 58 (2018) 082006.

*Provided by General Atomics and UC Irvine.*

#### 3.5.6. Gamma Ray Imager (GRI)

Andrey Lvovskiy ([lvovskiya@fusion.gat.com](mailto:lvovskiya@fusion.gat.com)), GA

*What it is for:* Gamma Ray Imager is a diagnostic designed to image the distribution of runaway electrons in the poloidal cross-section of DIII-D and its evolution in the course of time.

*What it basically does:* GRI measures the bremsstrahlung radiation from REs (generated when electrons pass charged nuclei and thus change their trajectories) in the gamma range (1–30 MeV) using a 2D array of scintillating gamma detectors.

*What it can also do, but do not use it for that:* GRI can also see losses of REs (when REs hit the wall, they produce bremsstrahlung radiation inside the material of the wall), but plastic scintillators and BGO array are more suitable for that.

*What it cannot do:*

- GRI sees almost no fast electrons below 1 MeV
- GRI is not designed to investigate hot ions
- GRI is sensitive to neutrons and thus cannot provide adequate measurements during continuous NBI

### 3.5.7. Outreach Ideas in EP physics

#### **Plasmoid injection using coaxial helicity injection**

- *Background:* plasmoids form when current layers tear and break, important in solar reconnection events
- *Method:* CHI can be done with external ‘guns’ and is traditionally for current drive in spheromaks and has been previously done on NSTX.
- *Possible Connections:* toroidal current drive or current profile manipulation by plasmoid injection, study of plasmoid formation in collisional plasma with high Lundquist numbers, different than experiments dedicated to reconnection
- *EP physics interest:* particles can be accelerated by reconnection events, current/plasma profiles can be manipulated to affect AE drive

#### **Energetic Particle Channeling**

- *Background:* waves could transfer energy from high energy particles (fast-ions or alphas) to low energy particles (ions) before they are lost (find a way to bypass collisional slowing down)
- *Method:* Waves can be launched or driven by population inversions in velocity space or real space. Use external antenna (probably have one in a closet somewhere?) to drive waves on purpose. Drive AEs? Mode converted Ion Bernstein waves?
- *Possible Connections:* Energetic particle channeling is of interest in astrophysics, including the properties of turbulent cascades from injected Alfvén waves, with relations to acceleration of cosmic rays, ion heating in the solar corona and solar wind, and structure formation in the solar wind through strong wave-particle resonance.
- *EP physics interest:* exploiting energy transfer to background ions could significantly enhance fusion performance

#### **Beam or laser driven wakefield particle acceleration**

- *Background:* Firing beam or laser pulses into a plasma at the plasma frequency will accelerate charged particles, where the accelerating field scales with the square root of the electron density.
- *Method:* Mount a wakefield particle accelerator on DIII-D and diagnose the spectrum of accelerated particles using ICE and gamma ray imager.
- *Possible Connections:* Wakefield accelerators are gaining attention with practical applications for the next generation of particle accelerators, and with laboratory astrophysics studies involving the generation of ultra-high energy cosmic rays or relativistic jet-plasma interactions.

### 3.6. Boundary Diagnostics

#### 3.6.1. Filterscopes

Aaron Sontag ([sontag@fusion.gat.com](mailto:sontag@fusion.gat.com)), ORNL

- Fast filtered visible spectral emission. Can be used for relative intensity of emission, primarily deuterium lines. (Also used for ELM timing.)  
Time resolution: usually sample every 50  $\mu\text{s}$ , can sample every 100  $\mu\text{s}$   
Spatial resolution: 2.5-4 cm diameter line-integrated chord,  $\sim$ 10-cm chord separation
- 8 vertical chords with 4-cm spot size spanning upper divertor, 16 vertical chords spanning lower divertor. All measure D- $\alpha$  (656 nm, 1 nm window) emission, many measure C III (465 nm, 3 nm window), a small subset of views measure C II, D- $\beta$ , D- $\gamma$ , He II, or Ne I emission.

#### 3.6.2. Multichordal Divertor Spectrometer (MDS)

Bob Wilcox ([wilcox@fusion.gat.com](mailto:wilcox@fusion.gat.com)), ORNL.

- Measures absolutely calibrated spectral emission. Can be used to determine presence of impurities, impurity density, ion temperature via Doppler broadening.
- Views a 7 nm wide spectrum  
Can be tuned to any central wavelength in the range: 385-720 nm  
Spectral resolution:  $\sim$ 0.02 nm  
Minimum integration time: 1 ms  
Spatial resolution: 2.5-4 cm diameter line-integrated chord,  $\sim$ 10-cm chord separation
- 7 vertical chords with 4-cm spot size spanning upper divertor; 6 vertical chords with 2.5-cm spot size spanning lower divertor; 7 2.5-cm tangential views in lower divertor; 1 radial midplane chord; 1 chord viewing upward into SAS divertor.

#### 3.6.3. Bolometer

Auna Moser ([mosera@fusion.gat.com](mailto:mosera@fusion.gat.com)), GA.

- Total radiated power. Crossed chord arrays are inverted to give 2D profile of radiated power (assumes toroidal symmetry and radiation constant on flux surface). Symmetric profile subtracted to get asymmetric (divertor) radiation.
- Radiated power range:  $\sim$ 0.01 W/cm<sup>3</sup> to  $\sim$ 10 W/cm<sup>3</sup>
- Time resolution:  $\sim$ 10 ms, usually use 40 ms integration time  
Spatial resolution: chord separation varies,  $\sim$ few to  $\sim$ 10 cm

#### 3.6.4. Divertor Thomson Scattering

Fenton Glass ([glassf@fusion.gat.com](mailto:glassf@fusion.gat.com)), GA.

- Provides  $n_e$ ,  $T_e$ ; can be used to calculate ion saturation current ( $J_{\text{sat}}$ ) and perpendicular heat flux ( $q$ ).
- 16 spatial locations are split between upper (12 or 4 locations) or lower divertor shelf (4 or 12 locations, respectively) at  $R = 1.485$  m.
- Instead of the 16 locations, 12 spatial locations can be made available at  $R = 1.335$  m in the lower divertor floor region.
- Spans up to  $\sim$ 22cm in lower divertor and  $\sim$ 25cm in upper divertor regions.

- Time resolution: measurement time window 10 ns, measurement time resolution 20 ms (50 Hz).
- Spatial resolution: measurement volume  $\sim 1 \times 0.3$  cm, measurement center separation 2-5 cm.
- Plasma can be swept horizontally past vertical array to build 2D profile of  $n_e$ ,  $T_e$ ,  $p_e$ .

**What is measured:**

Absolute electron temperature ( $T_e$ ) and density ( $n_e$ ) are measured in the divertor regions of DIII-D by quantifying the intensity and breadth of spectral broadening for a 1064 nm Nd:YAG laser traversing the plasma in a vertical arrays located in the upper and lower divertor region. Using DTS-measured  $T_e$  and  $n_e$  and simple plasma boundary theory, ion current ( $J_{\text{sat}}$ ) and perpendicular heat flux ( $q_{\perp}$ ) may be calculated at the plasma boundary and compared to Langmuir probes and infrared camera diagnostics. Data may be used to infer the convected power and mach flow velocity along magnetic field lines, and conditions in the divertor region compared to those at the edge of the core plasma using the core Thomson scattering system.

**Range of measurement:**

$T_e$ :  $\sim 0.1$  eV – 5 keV

$n_e$ :  $5 \times 10^{18}$  /m<sup>3</sup> –  $1 \times 10^{21}$  /m<sup>3</sup>

$p_e$ : 0.4 Pa – 100 kPa

**Region of measurement:**

Up to sixteen optically monitored measurement points spanning  $\sim 25$  cm in Z in the upper or lower divertor regions. Major radius of the array is either 1.335 or 1.485 m. Plasma may be swept horizontally through a discharge while keeping other parameters constant, and 1D DTS data through the sweep remapped to a single magnetic equilibrium to construct a 2D profile of  $T_e$ ,  $n_e$ , and  $p_e$ .

**Resolution of system:**

Measurement volume for each of the sixteen channels is up to  $\sim 1$  cm tall and 0.3 cm in diameter. Measurement period is defined by the duration of the laser pulse, 10 ns, and frequency of up to 50 Hz with a single 50Hz 1J/pulse laser operating in the system.

**Possible physics applications:**

DIII-D was the first tokamak in the world with a Thomson scattering system in the divertor region and currently has the most advanced measurement coverage, making it uniquely powerful to characterize divertor plasma. DTS has been used extensively to study conditions at the plasma-facing surface and operating scenarios compatible with long-term operation of future fusion devices. DTS is especially valuable for boundary code modeling and validation. The system has recently been used to study the impact of  $\mathbf{E} \times \mathbf{B}$  drifts on the plasma.

**Recent publications:**

F. Glass, *et al.*, "[Upgraded Divertor Thomson Scattering system on DIII-D](#)", Review of Scientific Instruments, **87**, (2016) 11E508

A.G. McLean, *et al.*, "[Electron pressure balance in the SOL through the transition to detachment](#)", Journal of Nuclear Materials, **463**, (2015) 533.

### Contact information:

Dr. Adam McLean, Lawrence Livermore National Laboratory (LLNL)

Email: [mclean@fusion.gat.com](mailto:mclean@fusion.gat.com) . Phone: 858-455-4122

#### 3.6.5. Fast neutral pressure (ASDEX) gauges

Morgan Shafer ([shafer@fusion.gat.com](mailto:shafer@fusion.gat.com)), ORNL.

- Measures neutral pressure, can be used for pumping rates and particle balance.
- Five locations:
  - Lower divertor, under shelf (lower cryo plenum)
  - Upper divertor, under inner dome (inner upper cryo plenum)
  - Upper divertor, behind outer slanted baffle (outer upper cryo plenum)
  - Upper divertor, on inner dome (behind tile)
  - Outer midplane (behind tile)
- Pressure range:  $\sim 10^{-6}$  T to  $10^{-3}$  T  
Time resolution: 1-10 ms

#### 3.6.6. Coherence Imaging Spectroscopy (CIS) flow camera

Cameron Samuel ([samuellc@fusion.gat.com](mailto:samuellc@fusion.gat.com)), LLNL.

- 2D image of ion velocity in the SOL and divertor region
- Two cameras:
  - Tangential view of lower divertor, detailed view of divertor legs and x-point.
  - Wide field of view “periscope” camera viewing full cross section, including upper and lower divertor.
- Velocity range: toroidal flows of 0-40 km/s.  
Spatial range: usually uses C III or He II which emit in regions with 10-40 eV, other lines/regions possible.
- Velocity resolution: relative velocity within shot  $\sim 0.3$  km/s, absolute velocity  $\sim 3$ -10 km/s.  
Temporal resolution: integration time 1 ms, sampling time 20 ms (periscope) or 2 ms (divertor).  
Spatial resolution: varies in field of view,  $\sim 1$  cm (periscope),  $\sim 1$  mm (divertor).

#### 3.6.7. IR cameras

Charles Lasnier ([lasnier@fusion.gat.com](mailto:lasnier@fusion.gat.com)), LLNL.

- Heat flux to wall, tile temperature.
- Three cameras:
  - Wide field of view “periscope” camera viewing full cross section, or 3X re-targetable view depending on installed optics
  - Vertical view of lower divertor.
  - Vertical view of DIMES, available in L-mode by request.
- Temperature range room temperature up to  $\sim 1100^\circ$  C.
- Spatial resolution:  $\sim 3$  mm/pixel lower divertor, sub-mm possible in DIMES-view L-mode only,  $\sim 1$  cm/pixel (periscope).
- Time resolution:
  - Lower divertor and DIMES-viewing cameras: 8 ms (2D full image), 80  $\mu$ s (lower

divertor radial lineout)  
Periscope: 1 ms for 2D full image 35  $\mu$ s vertical lineout.

### 3.6.8. Plunging probes (2)

Jose Boedo ([boedo@fusion.gat.com](mailto:boedo@fusion.gat.com)), UCSD.

Slow (100 ms) plunge but very fast (1 MHz) sampling of edge (~ 10 cm from wall) plasma electron density, electron temperature, potential, and flow. Provided by UCSD.

### 3.6.9. DiMES/MiMES

Dmitry Rudakov ([rudakov@fusion.gat.com](mailto:rudakov@fusion.gat.com)), UCSD.

Reciprocating sample manipulators to expose samples to boundary plasma from below or side of plasma. Very slow (one full shot exposure minimum, removed between shots). Provided by UCSD.

### 3.6.10. Divertor EUV/VUV Survey Spectrometer (DivSPRED)

Adam McLean ([mclean@fusion.gat.com](mailto:mclean@fusion.gat.com)), LLNL.

<https://diii-d.gat.com/diii-d/Divspred>

*Spatial:* About 1cm collection diameter at the shelf flow.

*Temporal:* Standard operating speed is 545Hz

### 3.6.11. Penning & Baratron Gauges

Ed Hinson ([hinsone@fusion.gat.com](mailto:hinsone@fusion.gat.com)), UW

[https://diii-d.gat.com/diii-d/Penning\\_gauge](https://diii-d.gat.com/diii-d/Penning_gauge)

The DIII-D Penning gauge system is used to detect impurities in the D3D pump ducts (upper outer, lower). The gauges are based upon a low temperature discharge maintained in a space connected to the pumping plenum. Line emission in the discharge is monitored with optical views equipped with filters for a specific species of interest. Total pressures as well as individual partial pressures of impurity species can be measured on time scales of the order 100ms, down to 1-10 utorr depending on the species and time scales required. Up to 3 species can be measured at each location simultaneously. A calibration must be performed before or after the experiment to determine the precise relationship between line emission and pressure.

To coordinate an impurity measurement during your experiment contact [hinsone@fusion.gat.com](mailto:hinsone@fusion.gat.com) sufficiently in advance of the experiment to confirm that appropriate filters for your species are available, and obtain new ones if necessary. The quality of filter will affect the achievable time scales and minimum detectable concentrations. The current inventory supports, in varying capacities, measurements of Ne, N, Ar, He, and D/H.

### 3.6.12. Fixed Langmuir probes

Jon Watkins ([watkins@fusion.gat.com](mailto:watkins@fusion.gat.com)), SNL.

<https://diii-d.gat.com/diii-d/DivProbes>

There are now seventy two (72) fixed Langmuir probes in the DIII-D divertor target plates which measure local density, temperature, particle flux, edge current, floating potential, and heat flux.

- Twenty high power "rooftop" probe tips are distributed along the lower divertor floor and shelf

- and twelve 6 mm diameter domed probes are mounted on the lower 45 degree tile and lower center post.
- There are thirty seven (37) domed probes and three (3) short rooftop probes mounted in the tiles of the upper divertor.

These probes are operated and maintained by [Sandia National Laboratories](#).

### 3.6.13. DiMES TV (Visible filtered imaging)

Tyler Abrams ([abramst@fusion.gat.com](mailto:abramst@fusion.gat.com)), GA.

<https://diii-d.gat.com/diii-d/DiMESTV>

DiMES TV provides high-resolution spectrally filtered imaging of the lower divertor surfaces. The current version of the system uses an EM-hardened PCO Pixelfly VGA 200/205 camera capable of 320x240 pixel resolution at 100 Hz, or 640x480 resolution at 50 Hz. A wide variety of lenses are available such that the system is capable of highly magnified views the DiMES sample exposure probe with extremely high (~1 mm) resolution, or imaging the entire lower divertor from the center post out to the edge of the divertor shelf; see more details on the [Views](#) page.

Typical applications of the DiMES TV camera system include spatially-resolved quantification of surface material erosion rates via the S/XB method, diagnosing the main ion or impurity radiation profile for validation with boundary physics models, studying the 2D divertor footprint patterns during the application resonant magnetic perturbations (RMPs), and imaging of material ejection events via dust mobilization and/or unipolar arcing.

A wide variety of band-pass filters are available for different applications. For a complete list of band-pass filters, see the [Filters](#) page. Before requesting DiMES TV for your experiment, it is recommended to discuss with the Diagnostic Operator about the optimal filter set, views, and spatial/temporal resolution for your experiment.

### 3.6.14. Wide Spectral Emission (WiSE) Spectroscopy

Adam McLean ([mclean@fusion.gat.com](mailto:mclean@fusion.gat.com)), LLNL.

<https://diii-d.gat.com/diii-d/WiSE>

The WiSE diagnostic is currently being commissioned. Once basic operating parameters are known, they will be posted

*Spatial:* About 1cm collection diameter at the shelf flow.

*Temporal:* Standard operating speed is 100 Hz

### 3.6.15. Fast Thermocouples

Jon Watkins ([watkins@fusion.gat.com](mailto:watkins@fusion.gat.com)), SNL.

(No wiki page)

### 3.6.16. Tangential TV

Max Fenstermacher ([Max.Fenstermacher@gat.com](mailto:Max.Fenstermacher@gat.com)), LLNL.

(No wiki page)

### 3.6.17. LLAMA (Lyman-alpha measurement apparatus)

Jerry Hughes ([jwhughes@psfc.mit.edu](mailto:jwhughes@psfc.mit.edu)), MIT.

The diagnostic consists of two pinhole cameras, with linear AXUV detectors that measure of profiles of Lyman-alpha emissivity across the HFS and LFS boundary.

Scientific goals: main chamber neutrals and ionization source; pedestal particle transport; divertor neutrals leakage.

Measurement location:  $Z = -0.75\text{m}$ , i.e. intermediate location between midplane and x-point in LSN configuration.

Coverage: 20 views at HFS and 20 views at LFS (horizontal).

Resolution:  $< 1\text{ cm}$  (horizontal views allow for direct Abel inversion of brightness into emissivity)

Time resolution:  $\sim 1\text{ kHz}$  (limited by SNR associated with common mode EM pickup).

Designed, installed and operated by as PPPL-MIT collaboration.

### 3.6.18. Tile Current Monitors

Andrey Lvovskiy ([Ivovskiya@fusion.gat.com](mailto:Ivovskiya@fusion.gat.com)), GA

The tile current array consists of an array of current shunts designed to measure the flow of open-field-line poloidal current (typically "halo" currents during disruptions). Presently the system provides only measurements through the bottom divertor shelf support legs.

### 3.6.19. Surface Eroding Thermocouples (SETCs)

Jun Ren ([renjun@fusion.gat.com](mailto:renjun@fusion.gat.com)), UTK

There is an array of 12 SETC being installed in the SAS divertor to provide the direct surface temperature measurement. The local incident heat flux is able to be calculated from measured surface temperature using a 1D finite difference thermal model.

Temperature range :  $0^\circ\text{C}$  up to  $2320^\circ\text{C}$

Temporal resolution : sensor thermal response  $< \text{few ms}$ , Standard operating speed is  $10\text{ kHz}$

Spatial resolution :  $< 1\text{mm}$

Modeling, Analysis and Simulation Tools

For more details on this section contact Sterling Smith ([smithsp@fusion.gat.com](mailto:smithsp@fusion.gat.com)), GA.

**An internal web page listing more codes and support links is available here:**

<https://diii-d.gat.com/diii-d/Software>

There are a number of analysis codes routinely used by DIII-D scientists for a variety of purposes. Each of the codes described below has potential pitfalls, and any results obtained from them should be vetted by an appropriately experienced researcher, possibly even the code maintainer proper. Codes that make use of a GUI require the -XY flags to be given to ssh. The current cluster is the iris cluster. The most efficient way to connect to the current cluster for using a GUI is with the NoMachine client connected to the cybele server.

### 3.7. General signal viewing

There is a variety of data signals that are recorded during each DIII-D discharge (see the section on diagnostics). Whether stored in PTDATA or MDS+, most data locations have a pointname – a unique name across the DIII-D data storage that allows that signal to be retrieved with a single variable name. Some pointnames are populated as the result of some between shot code being run. The status of codes run between shots can be viewed at <http://remis.gat.com/dam>

#### 3.7.1. Reviewplus

The reviewplus tool is designed for quickly retrieving and plotting pointnames or full MDS+ paths. It can be launched from the iris command line with ``module load defaults; reviewplus``. Signals to be plotted can be added from the “Edit->Signals” menu item. The current signals can be saved and then reloaded. The usual place to store these is `/fusion/projects/toolbox/reviewplus/<user>`, and it may be useful to start from one stored there already.

#### 3.7.2. OMFIT SCOPE module

The SCOPE module in OMFIT can display signals, similar to reviewplus.

#### 3.7.3. TRAVERSER

IDL GUI for viewing of the MDS+ trees, listing of available signals in MDS+ and listing of the supplemental information to the signals.

#### 3.7.4. pySpecview

Handy tool for investigation of spectrograms from all fast diagnostics available on DIII-D. It can be used to estimate M and N number of the mode from magnetics and locate mode from ECE or SXR data. More details are here: <https://diii-d.gat.com/diii-d/PySpecview>

### 3.8. Equilibrium

At the heart of all tokamak analysis is an equilibrium code, which solves the Grad-Shafranov equation for the magnetic equilibrium subject to external or internal measurements

### 3.8.1. EFIT

The EFIT code [Lao 1985], is the workhorse equilibrium reconstruction code for DIII-D. A version runs in real time to provide the model for the equilibrium, from which shape control is obtained. It also runs between shots using only external magnetics constraints (stored as EFIT01), and including external magnetics and internal Motional Stark Effect current constraints (stored as EFIT02). The equilibrium obtained from EFIT can be viewed using the `efitviewer` utility on the current cluster. Running EFIT is beyond the scope of this document, but the user can be guided by the `EFITtime` module GUI in OMFIT.

## 3.9. Profile fitting

The kinetic characteristics of the plasma – the densities, temperatures, and bulk velocities – are measured at a given R,Z location, or at a given magnetic field. It is common to map these points to a given equilibrium (where in the low rotation limit these kinetic quantities are constant on a flux surface). It is also common to fit a functional form to the quantity to obtain a continuous profile or to obtain characteristics of the fit such as the value at the magnetic axis (the “core” value), or the height or width of the pedestal, if any. There are two sets of analyses that run automatically – TANH and ZIPFIT – and there are a plethora of other tools that can be used for manual profile fitting.

### 3.9.1. TANH

The TANH profile fitting routines attempt to fit the electron temperature and density measured by Thomson Scattering to a modified hyperbolic tangent functional form in real space (not mapped to an equilibrium). The pedestal top values are stored as `prmtan_neped`, `prmtan_teped`, and `prmtan_peped`, and the widths (in real space) as `prmtan_newid`, etc..

See [https://diii-d.gat.com/diii-d/Ts\\_pointnames](https://diii-d.gat.com/diii-d/Ts_pointnames)

### 3.9.2. ZIPFIT

The electron density and temperature measured by Thomson Scattering, the electron temperature measured by ECE, and the impurity ion temperature, velocity, and density measured by CER are mapped to an equilibrium (usually EFIT01), and then fit with a couple of functional forms, where the fit with the best value of  $\chi^2$  at each time slice is kept and stored in the ZIPFIT01 tree of MDS+. There is a `zipfit_viewer.py` utility available with ``module load pyepd`` on iris.

More information at <https://diii-d.gat.com/diii-d/Zipfituser>

### 3.9.3. QUICKFIT

Fast and simple tool for investigation and fitting of the kinetics profiles. It uses 2D Gaussian process regression to obtain radial and temporal evolution of the fitted quantities and their uncertainties. Current version supports fitting of charge exchange  $T_i$  and  $\omega$  data, Thomson scattering  $n_e$ ,  $T_e$  and  $n_e$  from reflectometer and  $\text{CO}_2$  interferometer. Impurity density from CER and SPRED can be either loaded from IMPCON or calculated internally. The local  $Z_{\text{eff}}$  profile is calculated from line-integrated measurements of visible bremsstrahlung, the filterscope array, and from the background of CER spectra. More details here: <https://diii-d.gat.com/diii-d/Quickfit>  
QUICKFIT can be also loaded as a module in OMFIT.

#### 3.9.4. OMFITprofiles

The OMFITprofiles module in OMFIT was born to provide advanced data filtering and fitting options with both core and edge focused capabilities. Please see its tutorial linked from its module page at the OMFIT webpage <https://gafusion.github.io/OMFIT-source/modules.html>.

#### 3.9.5. Pyped toolkit

The pyped toolkit was created to run a variety of codes and fit profiles in a way that was best suited for pedestal analysis, including ELM filtering. The tools are available with `module load pyped` on iris. More documentation is at the website <https://diii-d.gat.com/diii-d/PyD3D>

#### 3.9.6. GAprfiles

The GAprfiles suite of fitting tools exists as the first fitting tool available for profile fitting at DIII-D. It is available on iris as gAprfiles after `module load defaults`. There is some functionality available in GAprfiles which is not yet available in other fitting tools, but if that is the case, then it would be preferable to create that functionality in the newer tools, as the large spaghetti codebase of GAprfiles is making it hard to maintain, and it will become deprecated at some point in the future.

#### 3.9.7. pyTomo

Tomographic inversion GUI for SXR and bolometers in DIII-D. It uses Minimum Fisher regularisation and anisotropic smoothing based on real magnetic equilibrium to create a high fidelity reconstructions of the 2D emissivity profiles. More documentation is at the website <https://diii-d.gat.com/diii-d/PyTomo>

#### 3.10. Source deposition

The main actuators for changing the conditions in DIII-D, such as the neutral beams, the electron cyclotron waves, pellets, ohmic heating, and gas puffing require some type of computation to obtain their deposition into the plasma.

##### 3.10.1. ONETWO and AutoONETWO

The ONETWO code was originally developed as a transport code, including the calculation of deposition from ohmic, NBI, EC, and bootstrap sources. The ONETWO code is run automatically between discharges in power balance mode under the name autoONETWO based on the EFIT02 equilibria and ZIPFIT01 profiles and the results are stored in the AOT01 MDS+ tree.

##### 3.10.2. TRANSP

The TRANSP code is similar to ONETWO, but has a greater range of features. Running TRANSP is most easily accomplished via the TRANSP module in OMFIT.

#### 3.11. Integrated modeling tools

In addition to the codes specifically mentioned above, there are a few software suites, which attempt to provide a more unified approach to data analysis and code workflows.

##### 3.11.1. OMFIT

OMFIT – One Modeling Framework for Integrated Tasks – is the most widely used integrated modelling tool for fusion research in the world. As of Oct 2021, there were over 1000 users worldwide from a variety of devices, including DIII-D, NSTX-U, C-Mod, JET, MAST-U,

KSTAR, COMPASS, TCV, and ASDEX-U. 85 individuals from 29 institutions have contributed to OMFIT. Instructions for running OMFIT on the iris (or forthcoming omega) cluster are at <https://gafusion.github.io/OMFIT-source/installations/GA.html> . Below are mentioned a few more modules (in addition to those referenced in previous subsections) that may be of interest to general DIII-D analyses.

The full list of modules is at <https://gafusion.github.io/OMFIT-source/modules.html> .

#### 3.11.1.1. kineticEFITtime

The kineticEFITtime module of OMFIT links together equilibrium reconstruction, profile fitting, bootstrap current calculation, and fast ion calculation, to provide pressure and current constraints for so-called “kinetic EFIT” equilibrium reconstructions. This module’s linkages also provide a convenient method of running TRANSP and ONETWO for power balance.

#### 3.11.1.2. Boundary Toolbox

Similar to the usefulness of the linking in the kineticEFITtime module, there is a usefulness to having a grouping of modules of interest for boundary or scrape off layer analysis, such as strike point analysis and an indication of the level of detachment.

#### 3.11.2. efitviewer overlays

Within the efitviewer tool, there exists the option to bring up a diagnostic overlay window. Some of the overlay options are really tools for running other codes. Such are the case for echres and nbipLOT, where these are tools using ZIPFIT as input by default for running TORAY and NUBEAM (through ONETWO) respectively, and are useful for evaluating current and future setups for NB voltages and EC aiming.

Further information at [https://diii-d.gat.com/d3d-wiki/images/9/92/Intro\\_to\\_DIII-D\\_tools.pdf](https://diii-d.gat.com/d3d-wiki/images/9/92/Intro_to_DIII-D_tools.pdf)

#### 3.11.3. pyped (Osborne tools)

As mentioned under profile fitting above, the pyped toolkit is optimized for looking at the pedestal. It can assist in kineticEFIT reconstructions and pedestal stability analysis.

The full documentation is at <https://diii-d.gat.com/diii-d/PyD3D>

## 4. Planning Experiments

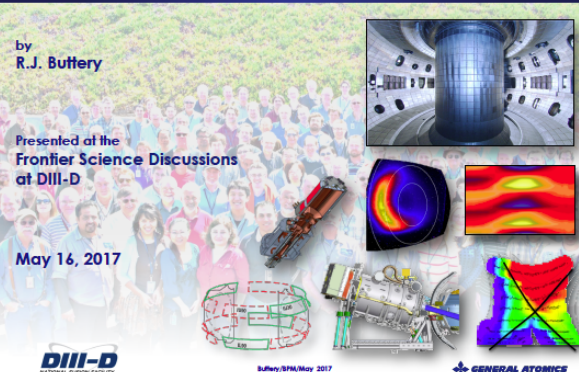
Richard Buttery ([buttery@fusion.gat.com](mailto:buttery@fusion.gat.com)), GA.

### Preparation of Experiments at DIII-D

by  
R.J. Buttery

Presented at the  
Frontier Science Discussions  
at DIII-D

May 16, 2017



**DIII-D**  
NATIONAL FUSION FACILITY

Buttery/BPM, May 2017

GENERAL ATOMICS

### Objectives and Initial Considerations in Preparing Experiments

- **Need to work out what we can do on DIII-D and approximate approach**
  - Clear identification of physics goals and testable hypothesis
  - What results plots do you want to make?
- **What can DIII-D do?**
  - An iteration between goals and machine capabilities
    - Hardware/plasma manipulation
    - Diagnostics
  - Need to talk a lot to people
- **Max needs to know what systems you need soonish**
- **Should also develop rough shotplan (what scans you want to do, approximate parameters and techniques)**
- **Then move to formal shot plan and settings...**



2 - Buttery/BPM, May 2017

xxx-1TR,8ly

### Key Steps in DIII-D Experiment preparation

- **Early stage: Max's 20 hardware questions**
  - <physics discussion on context, possibilities, goals>
  - <develop draft "miniproposal" shot plan – upload it>
  - <good idea to document some projections on expected behavior if this is testing a code>
- **~4 weeks before experiment: Review shot plan amongst a group of relevant experts & document in MP system**
  - <update miniproposal accordingly>
  - <MP upload includes filling out/updating hardware and diagnostic settings>
- **By COB Monday 2 weeks before experiment: upload completed miniproposal & set ready for review**
  - <formal review by a group leader, chief operator and run coordinator. Run coord notifies operations of needs>
- **Run the experiment!**



3 - Buttery/BPM, May 2017

xxx-1TR,8ly

### Design of a Miniproposal

1. **Introduction should set key testable hypothesis – something you can judge whether or not you have succeeded by**
2. **Background – motivation, past data**
3. **Approach – description of your main methods and logic, discussion of options and needed**
  1. Draw in some waveforms and show a reference shot if appropriate
4. **Resources – describe all the setting for hardware and diagnostics**
5. **Shot plan – numbered list of shots, grouped into scans**
  1. Flag decision points and contingencies
  2. Estimate number of shot at each step. Include possible tuning shots. Note principle setting changes
6. **Radiation estimate**



4 - Buttery/BPM, May 2017

xxx-1TR,8ly

### Tips on Miniproposal

- **Have a clear idea of what you are testing.**
- **Think about what results plot you will make**
  - How will this answer the physics question
- **Talk to experts about what can be done**
- **Need to clearly know design of shots, and anticipate scan points and contingencies in advance**
- **Experiments are very fluid, you will likely depart from shot plan rapidly, improvising around it in light of data taken**
  - but remember to consult it – it can help you connect back to your plan!



5 - Buttery/BPM, May 2017

xxx-1TR,8ly

### Preparation for the Experiment Day

- **Need to learn key shot logging and data visualization tools**
  - Develop a "standard set" of things to look at
  - We will partner you with people who can show you how, but good for you to be able to do this.
- **Talk to relevant experts to prepare for the day**
  - Work with diagnostic coordinator and prospective physics operator (person who codes machine control to deliver shots)
  - Speak to key diagnostic leaders you will rely on
- **Prepare details**
  - Waveforms, diagnostic settings, contingencies
- **Prepare an 805 talk**



6 - Buttery/BPM, May 2017

xxx-1TR,8ly

## On Experiment Day

- Get logged into data and logging systems
- Give 5 minute "8:05" presentation on ~1 slide context, 1-2 slides on cartoon method, 1-2 slides summarized shot plan, 1-2 slides key settings
- Have copies of shot plan ready
- Buy donuts!
- Start shots after reference shot (usually around 8:40)
- Shots will run every 15 minutes!
  - Try to decide next shot, one in advance
  - Use your standard set to look at key things.
  - Work out what you will need to check to decide next shot
  - Ask people to analyse stuff for you
- Get some pictures of key results through the day
- Prepare an 805 summary for next day: check off progress vs plan, note main technical issues, show some results snapshots, note value of any additional time



7 - Buttery/SPM/May 2017

xxz-17R,Bjy

## After the Experiment Day

- Give an 805 report the next day
- Later give a Friday science meeting summary
- Hold in depth discussion with your physics team on the results
  - plan the analysis, hand out tasks
- Review analysis and conclusions of work
- Prepare and review outputs (papers, talks)
- Publish!



8 - Buttery/SPM/May 2017

xxz-17R,Bjy

## Other Issues To Consider

- Carbon walls absorb and release gas, so this can influence conditions
- Grouping of studies with different toroidal field directions



9 - Buttery/SPM/May 2017

xxz-17R,Bjy

## 5. Mini-proposal Template

Richard Buttery ([buttery@fusion.gat.com](mailto:buttery@fusion.gat.com)), GA.

See next page for an example document that we use to specify everything we need to know to execute an experiment on the facility.

Date Approved: \_\_\_\_\_ By: \_\_\_\_\_

General Atomics

## DIII-D Mini-Proposal

Subject: <Title of experiment>

D3DMP No. 2018-XX-xx

revision x

From: <Author list>

Date: XXX XX, 2018

Revised: <date>

---

### 1. Purpose of Experiment (typically 1/3<sup>rd</sup> page of text + sketches if applicable)

Physics hypothesis to be tested or key advance aimed for: *this might include an operational goal (whether a particular technique can achieve a specified results) and/or a physics goal (eg resolving a give mechanisms of how one behavior can influence another)*

Principle result plots: *<provide description or cartoon>*

Impact: *<Describe how this result will inform future research in this area and the impact of this work on the path to fusion energy>.*

Predict first: *<Predictions from theory or simulation about the expected result of this experiment (if applicable). 1 or 2 sentence summary here, any figures in appendix>:*

Additional scientific goals or piggy-back studies:

### 2. Background *<~1 page should be plenty – key point is to help understand why the particular approach used here is being pursued, not to motivate getting run time>*

*<Motivate the studies – the challenge faced by future reactors, recent work in the field highlighting where we have got, particular roadblocks, promising techniques that may be adopted here.>*

<What is particularly important to get from DIII-D in this study, now? (what does DIII-D uniquely bring? What facet is timely and why?)>

**3. Experimental Approach** <1-2 pages is plenty, but take enough space to explain rationale for key choices in approach, decision points, and to provide an overview description of the techniques used.>

<Color code open issues that need to be fixed before run day in red.>

Describe the approach to be applied, what techniques to use, parameters to be scanned.

- Give a reference shot if possible, explain how it will be adapted.
- Provide diagram of time traces of key parameters for discharge design (if appropriate).
- Discuss rationale for choice of techniques to be applied and parameter settings.

Layout (at a high level – not the detailed shot plan order) the logic of the progression of stages in the experiment and the physics addressed by each. Note any decision points or branches in path.

Flag any pitfalls or aspects that may need additional time or contingency planning (eg if modes strike, or effect you are looking for does not manifest as expected)

Analysis & Roles:

Flag any elements requiring calculation or analysis prior to experiment. Note who will do them.

Provide list of roles for executing the experiment on the day, and who will do them.

Provide list of analysis tasks to be pursued after experiment completed, and who will do them (please also review analysis needs with your physics area meeting, once experiment has been run).

**4. Resources** <~1/2 page or so. Data on these systems is entered directly into the MP webpage, but note here explanatory/descriptive comments, or data needed for review.>

**4.1. Tokamak**

Shape, reference shot number, patch panel number,  $B_r$  range,  $I_p$ , directions, machine conditions needs and boronization. Identify physics operator.

## **4.2. Neutral Beams**

Sources, voltages, on/off axis, any special duration or modulation requests. PCS feedback. Identify beam programmer.

## **4.3. ECH**

Number of gyrotrons, minimum & desirable power needed, duration, modulation, control mode, special control algorithms. Identify ECH programmer

## **4.4. Diagnostics**

Any special issues needing description, plus link to MP diagnostic settings page (note essential/desirable/important system – essential means you don't run if unavailable; provide justifications for systems that require high time commitment). Identify diagnostic coordinator.

## **4.5. Gas Systems**

Setup, which gases, which valves, any particularly control. All unused gas lines should be evacuated before experiment commences.

## **4.6. Cryopumps**

Which cryopumps (all?), how long, He/N cold/room temp for each? Defrost during glow?

## **4.7. IC-coil requirements**

Which power supplies needed. Which coils. Current levels. Special control. Error field correction arrangements. Add link map in appendix.

## **5. Experimental Plan**

*<Describe each step conceptually with a phrase. Detail settings, parameters, scan point numerical values. Add time trace sketches if helpful. For each step provide a realistic estimate of number of shots (including if this typically takes >1 shot to tune discharge or avoid a pitfall).>*

### **1. Stage 1 description based on shot xxxxx (2 – 12 shots)**

<Notes...>

1.1. Dial up reference. (2 shots)

1.2. <describe a step or scan> (4-6 shots)

1.3. Contingence step (if undesirable event happens) (0-2 shots)

**2. Stage 2 description (4-14 shots)**

2.1. Step 1 (2 shots)

2.2. Step 2

2.3. ...

*(Decision point: Describe if next step might depend on what seen in above steps.)*

**3. Stage 3: (0-8 shots).**

3.1. Step 1

3.2. Step 2

3.3. ...

**3.4.**

*At this point we have met our main goal – following points desirable for documentation, more complete measurement or useful extensions*

4. Step description (2 shots)

5. ...

**Total**

**20-38 shots**

**6. Analysis Plan and Deliverables** <1/3<sup>rd</sup> page plus sketches>

*<Specify the anticipated publishable plot(s) to be derived from the experiment.*

*Give details of the elements of an analysis plan (data analysis, code simulations etc.) that will lead to generating the plot(s) and publication(s).*

*Record any plans for publication if the experiment is successful (people, conferences, papers).>*

## 7. Radiation Awareness

A site boundary limit of 600  $\mu\text{rem}$  is requested.

### **Appendix: 'Predict First' Predictions** (if applicable)

*<Paste in any plots, slides, quotes from papers, or table from work that uses theory or simulation predict specific results expected in this experiment.>*

## 6. Acknowledgements

This material is based upon work supported by the U.S. Department of Energy, Office of Science, Office of Fusion Energy Sciences, using the DIII-D National Fusion Facility, a DOE Office of Science user facility, under Awards DE-FC02-04ER54698. DIII-D data shown in this paper can be obtained in digital format by following the links at [https://fusion.gat.com/global/D3D\\_DMP](https://fusion.gat.com/global/D3D_DMP)

Disclaimer: This report was prepared as an account of work sponsored by an agency of the United States Government. Neither the United States Government nor any agency thereof, nor any of their employees, makes any warranty, express or implied, or assumes any legal liability or responsibility for the accuracy, completeness, or usefulness of any information, apparatus, product, or process disclosed, or represents that its use would not infringe privately owned rights. Reference herein to any specific commercial product, process, or service by trade name, trademark, manufacturer, or otherwise does not necessarily constitute or imply its endorsement, recommendation, or favoring by the United States Government or any agency thereof. The views and opinions of authors expressed herein do not necessarily state or reflect those of the United States Government or any agency thereof.